CHRONOLOGY OF HESPERIA PLANUM, MARS USING IMPACT CRATERS AS STRATIGRAPHIC MARKERS. S.C. Mest[1,2], D.A. Crown[1], and D.C. Berman[1], [1]Planetary Science Institute, Tucson, AZ (mest@psi.edu); [2]NASA Goddard Space Flight Center, Greenbelt, MD.

Introduction: Impact craters represent temporally and stratigraphically distinct events in the geologic record of a planetary surface, can be used to constrain geologic history, and allow relative and absolute ages of geologic materials to be determined. In Hesperia Planum (HP), model ages derived for impact crater materials are being used to provide important temporal constraints on emplacement of the ridged plains material, ridge-forming events, and fluvial modification of the plains. This abstract presents initial results obtained from analyses for several impact craters in the Hesperia Planum region of Mars.

Geologic Setting: Hesperia Planum encompasses >2 million km^2 and is characterized by a high concentration of mare-type wrinkle ridges and ridge rings [1-4]. Most of HP occurs between 1000 and 2000 meters in elevation, but the southeastern part contains the depression of Eridania Planitia (0-1000 m elevation). The ridged plains of HP are stratigraphically significant and have been used to define the base of the Hesperian System [1,5]. Recent mapping studies at local [6-8] and regional [e.g., 2,9-12] scales have recognized areas within HP that do not conform to the characteristics of typical "ridged plains" and appear to have been formed or at least modified by fluvial processes. As a result, large areas of ridged plains within HP have been reclassified, suggesting a more complex and diverse geologic history.

Approach: This study involves compiling crater size-frequency distribution statistics for ejecta and floor deposits for relatively fresh craters in HP that could serve as important stratigraphic markers. Similar studies have been conducted in Deuteronilus Mensae [13,14] and have provided temporal constraints on the formation of the highland-lowland boundary, fretted terrain development, and emplacement of lobate debris aprons. In this study, craters are selected that are greater than 15 km in diameter, are isolated (from adjacent craters) and display pristine morphologies with little surface modification, and have sufficient coverage by high-resolution images. The availability of new high-resolution images allows us to characterize crater populations at diameters as small as 50 m for determination of relative (Martian time stratigraphic system) and absolute ages.

Data: We are using several high-resolution datasets to map materials associated with specific craters, as well as identify and measure superposed craters in order to compile crater size-frequency distribution statistics. The THEMIS daytime IR mosaic (100 m/pixel) serves as the regional base, supplemented by CTX (~5 m/pixel) and THEMIS VIS (~18 m/pixel) images; HiRISE (~1-2 m/pixel) and MOC (~2-12 m/pixel) images are being utilized in specific locations as needed.

Crater Mapping and Determination of Crater Size-Frequency Distributions: For each crater selected for analysis, images are processed in ISIS and imported into ArcGIS. The margins of the continuous ejecta blanket and crater floor deposits are digitized, and the diameters of superposed craters are measured. ArcGIS is being used to calculate unit areas and record crater diameters. Crater size-frequency distribution statistics are compiled using the methodology described in [15-18]; all impact craters (primaries and isolated secondaries) on a given surface are counted while avoiding areas that show obvious secondary rays, chains or clusters. These data are plotted on isochrons [16-18] to assess relative age (Martian time-stratigraphic age) and estimate absolute age. The production function used to determine the isochrons includes both primaries and a component of "background" secondaries (i.e., those secondaries not included in rays, chains or clusters) [16-18]. Cumulative crater statistics (i.e., N(2) and N(5), [7]) are also determined for comparison to statistics compiled IN previous geologic mapping studies [e.g., 1,2,6,7].

Results: We have identified 43 craters in HP for analysis (Fig. 1). Currently, we are focused on evaluation of three craters that are located within the central and eastern parts of HP.

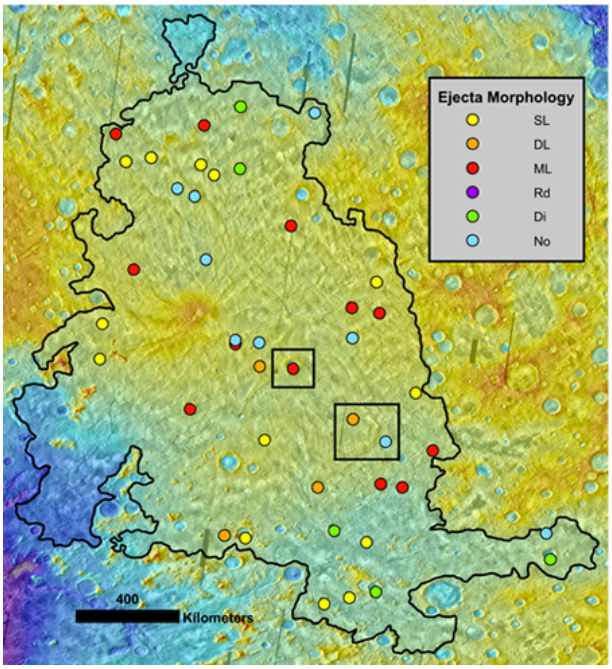

Figure 1. Map of HP (black boundary) and 43 pristine craters; 'Ejecta Morphology' defined by [19,20]. Black boxes indicate locations of (A) crater Kinkora and (B) two unnamed craters.

Two unnamed craters (Fig. 2), both ~15 km in diameter and located just north of Eridania Planitia, have had their ejecta blankets mapped and all craters (D>50 m) superposed on their ejecta blankets, rims, and floors counted using CTX images. Crater 1 exhibits Double-Layer ejecta morphology [19,20] and contains 187 superposed craters. Crater 2 has 'No' ejecta classification [19,20], but clearly displays morphology that could be classified as Single- or Double-Layer ejecta and contains 88 superposed craters. After binning the crater count data (Fig. 2), both craters exhibit mid-Hesperian to Late Amazonian formation ages; the rollover is likely due to burial of smaller diameter craters by eolian materials.

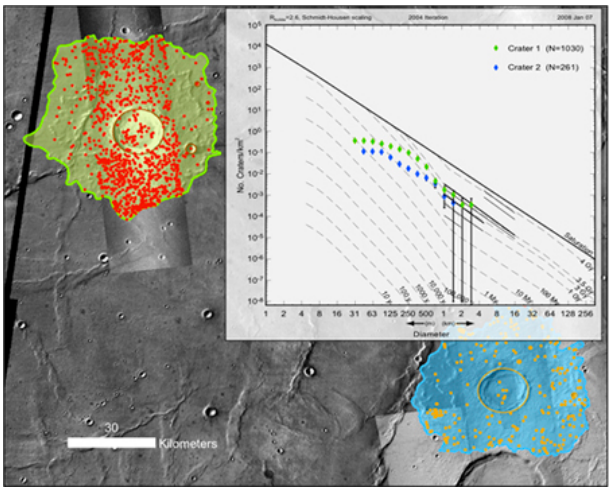

Figure 2. Map of two craters (D~15 km) in south central HP with lobate ejecta morphologies [19,20] showing their ejecta deposits and superposed craters used to derive crater size-frequency distribution plots (inset). Base includes CTX images (~5 m/pixel) and THEMIS day IR mosaic (512 ppd).

The third crater, Kinkora (D=47 km; Fig. 3a), is located ~400 km southwest of Tyrrhenus Mons. Kinkora's ejecta blanket has been mapped and exhibits Multi-Layer ejecta morphology [19,20]. All craters (D>100 m) superposed on its ejecta blanket, rim, and floor have been counted (N=2040). Here, CTX images, supplemented by THEMIS VIS images, were used for crater identification and distinction between primary and secondary craters. Preliminary counts using superposed craters greater than 500 m (Fig. 3b), identified in only the THEMIS daytime IR mosaic and in individual THEMIS VIS images, show a strong fit to the Noachian-Hesperian boundary, which is consistent with regional and local mapping studies. For example, recent mapping of southern parts of Hesperia Planum by [6] has shown that the plains are Early Hesperian to Late Noachian in age and that a significant amount of post-plains emplacement fluvial modification, estimated by the ages of large (D>25 km) superposed craters, Early to mid-Hesperian.

Summary: High-resolution images are providing important constraints on the relative ages of fresh impact craters. The results of this study are being used to constrain the ages of the underlying plains materials within HP and evaluate the timing of wrinkle ridge formation within the plains. Dating multiple craters throughout HP will also enable us to evaluate hypotheses for the origin(s) of reclassified HP materials.

References: [1] Greeley, R., and J.E. Guest (1987) USGS Misc. Inv. Ser. Map, I-1802-B. [2] Tanaka, K.L., and G.J. Leonard (1995) *JGR*, **100**, 5407-5432. [3] Potter, D.B. (1976) USGS Geol. Invest. Ser. Map I-941, 1:5M scale. [4] King, E.A. (1978) USGS Geol. Invest. Ser. Map I-1073. [5] Tanaka, K.L. (1986) *JGR Suppl.*, **91**, E139-E158. [6] Mest, S.C., and D.A. Crown (2002) USGS Geol. Inv. Ser. Map I-2730. [7] Mest, S.C., and D.A. Crown (2003) USGS Geol. Inv. Ser. Map I-2763. [8] Mest, S.C. and D.A. Crown (2012) *Geologic Map of MTM -30247, -35247 and -40247 Quadrangles, Reull Vallis Region Of Mars*, USGS, in review. [9] Crown, D.A., et al. (1992) *Icarus*, **100**, 1–25. [10] Mest, S.C., and D.A. Crown (2001) *Icarus*, **153**, 89-110. [11] Gregg, T.K.P., and D.A. Crown (2009) NASA/CP—2010–216680, 27-28. [12] Ivanov, M.A., et al. (2005) *JGR*, **110**, E12S21, doi:10.1029/2005JE002420. [13] Berman, D.C., et al. (2011) 42nd LPSC, **#1435**. [14] Joseph, E.C.S., et al. (2011) 42nd LPSC, **#1206**. [15] Berman, D.C. and W.K. Hartmann (2002) *Icarus*, **159**, doi:10.1006/icar.2002.6920. [16] Hartmann, W.K. (2005) *Icarus*, **174**, 294-320. [17] Hartmann, W.K. (2007) 7th Intl. Conf. on Mars, **#3318**. [18] Hartmann, W.K. (2007) *Icarus*, **189**, 274-278. [19] Barlow, N.G. (2003 6th Intl. Conf. on Mars, **3073**. [20] Barlow, N.G. (2006) 37th LPSC, **#1337**.

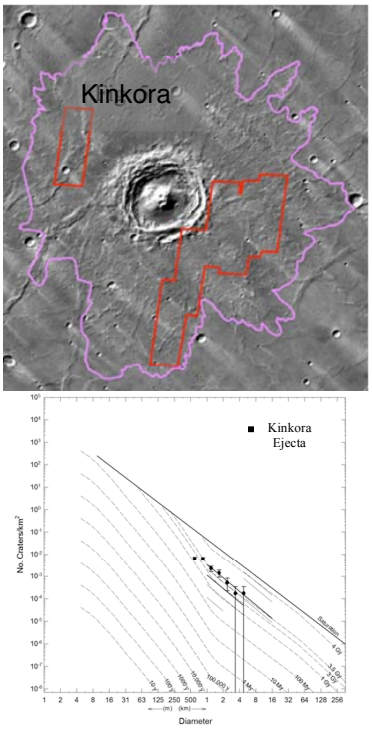

Figure 3. (a) THEMIS daytime IR mosaic of Kinkora crater with ejecta (outlined in purple). Red boxes show the locations of THEMIS VIS images used for crater counts. (b) Crater size-frequency distribution for the part of the ejecta blanket of Kinkora found within the red boxes shows a fit to the Noachian-Hesperian boundary over most of the size range measured (500 m to 5 km).